



# A Ketogenic Diet Improves Mitochondrial Biogenesis and Bioenergetics via the PGC1 $\alpha$ -SIRT3-UCP2 Axis

Md Mahdi Hasan-Olive<sup>1,2,3</sup> · Knut H. Lauritzen<sup>1,4</sup> · Mohammad Ali<sup>5</sup> · Lene Juel Rasmussen<sup>3</sup> · Jon Storm-Mathisen<sup>1</sup> · Linda H. Bergersen<sup>1,2,3</sup> 

Received: 7 January 2018 / Revised: 20 June 2018 / Accepted: 24 June 2018 / Published online: 19 July 2018  
© Springer Science+Business Media, LLC, part of Springer Nature 2018

## Abstract

A ketogenic diet (KD; high-fat, low-carbohydrate) can benefit refractory epilepsy, but underlying mechanisms are unknown. We used mice inducibly expressing a mutated form of the mitochondrial DNA repair enzyme UNG1 (mutUNG1) to cause progressive mitochondrial dysfunction selectively in forebrain neurons. We examined the levels of mRNAs and proteins crucial for mitochondrial biogenesis and dynamics. We show that hippocampal pyramidal neurons in mutUNG1 mice, as well as cultured rat hippocampal neurons and human fibroblasts with H<sub>2</sub>O<sub>2</sub> induced oxidative stress, improve markers of mitochondrial biogenesis, dynamics and function when fed on a KD, and when exposed to the ketone body  $\beta$ -hydroxybutyrate, respectively, by upregulating PGC1 $\alpha$ , SIRT3 and UCP2, and (in cultured cells) increasing the oxygen consumption rate (OCR) and the NAD<sup>+</sup>/NADH ratio. The mitochondrial level of UCP2 was significantly higher in the perikarya and axon terminals of hippocampus CA1 pyramidal neurons in KD treated mutUNG1 mice compared with mutUNG1 mice fed a standard diet. The  $\beta$ -hydroxybutyrate receptor GPR109a (HCAR2), but not the structurally closely related lactate receptor GPR81 (HCAR1), was upregulated in mutUNG1 mice on a KD, suggesting a selective influence of KD on ketone body receptor mechanisms. We conclude that progressive mitochondrial dysfunction in mutUNG1 expressing mice causes oxidative stress, and that exposure of animals to KD, or of cells to ketone body in vitro, elicits compensatory mechanisms acting to augment mitochondrial mass and bioenergetics via the PGC1 $\alpha$ -SIRT3-UCP2 axis (The compensatory processes are overwhelmed in the mutUNG1 mice by all the newly formed mitochondria being dysfunctional).

**Keywords** Ketogenic diet · MutUNG1 · Biogenesis · Bioenergetics

## Introduction

Mitochondria are of central importance for the complex processes of neurotransmission, neuronal plasticity, and energy homeostasis of neurons [1]. Energy demand is higher in neurons than in most other cells, which is reflected by high consumption of oxygen in the brain. Endogenous reactive oxygen species (ROS), arising from normal oxygen metabolism,

are mainly produced in mitochondria. ROS may lead to oxidative stress (OS) and mitochondrial DNA (mtDNA) damage, and ultimately in neurodegenerative pathology. Damage to the mtDNA and associated OS during neurodegenerative processes can impair neuronal energy homeostasis [2]. The frequency of oxidative damage of mtDNA is ten to 20 times greater than that of nuclear DNA [3]. Therefore, mitochondria need to have efficient DNA repair systems in order to maintain an error-free mitochondrial genome and to prevent dysfunction of the organelles [4, 5]. In base excision repair, uracil-DNA glycosylase (UNG) removes unnatural uracil from DNA [6], UNG1 being the mitochondrial form of the enzyme.

A ketogenic diet (KD) is a high fat, low carbohydrate and restricted protein diet that is beneficial for treatment of drug-resistant epilepsy [7–12]. This diet has also been proposed as a therapeutic diet in several neurological

**Electronic supplementary material** The online version of this article (<https://doi.org/10.1007/s11064-018-2588-6>) contains supplementary material, which is available to authorized users.

✉ Md Mahdi Hasan-Olive  
m.m.hasan@medisin.uio.no

✉ Linda H. Bergersen  
l.h.bergersen@odont.uio.no

Extended author information available on the last page of the article

diseases such as autism [13], amyotrophic lateral sclerosis [14], Huntington disease [15], Alzheimer's disease [16], and Parkinson's disease [17]. A KD mimics the metabolic state of long-term fasting by fatty acids being oxidized to ketone bodies. Ketone bodies produced in the liver act as an alternative energy source, compensating for limited availability of glucose during fasting [18]. Proposed hypotheses for the modes of action of KD are (1) lowering the blood pH, (2) shifting from glucose-based to ketone-based metabolism to produce more ATP [19], and (3) upregulating GABAergic inhibition [20]. Notably, a KD reduces midlife mortality and improves memory in aging mice [21, 22]. However, the molecular mechanisms underlying neuroprotective and anticonvulsant effects of KD are yet to be elucidated. Beta-hydroxybutyrate ( $\beta$ HB), and other ketone bodies, can cross the blood brain barrier (BBB) through monocarboxylate transporters (MCTs) [23] into the brain parenchyma for metabolism in brain cells and interaction with the  $\beta$ HB receptor, G-protein coupled receptor 109a (GPR109a, also known as HCAR2). A KD or  $\beta$ HB upregulate MCT1 [24], but the molecular regulation of  $\beta$ HB's receptor is yet to be investigated.

Uncoupling proteins (UCPs) regulate fatty acid metabolism. The proton conductance of UCP2 is sensitive to fatty acids and ROS [25]. Ketone bodies can increase the level of UCP2, reducing oligomycin-mediated ROS production in mouse hippocampus [26]. An excessive mitochondrial membrane potential causes a disproportionately large amount of ROS production [27]. This can be counteracted by increasing the level of UCP2 [28], which reduce the mitochondrial membrane potential through uncoupling, thereby lowering the kinetic rate of the electron transport chain, in addition to inducing an increase in the number of mitochondria, which thereby avoids compromising ATP production [29, 30]. Thus, UCP2 plays a positive physiological role in neuroprotection [29, 31] and aging [32–34]. UCP2 has been proposed as a novel neuroprotector in different neuropathologies, including Parkinson's disease [35, 36], epilepsy [29], and stroke [37].

A KD increases mitochondrial density in neuronal processes in the rat hippocampus [38]. Notably, the diet also raises mitochondrial proteins and UCP1 in mice [39]. The cytosolic and mitochondrial protein acetylation in liver is affected by a KD [40]. Moreover, ketone bodies protect mice against ischemic stroke by upregulating the mitochondrial  $\text{NAD}^+$ -dependent deacetylase sirtuin 3 (SIRT3) [41], which deacetylates numerous mitochondrial proteins to regulate mitochondrial functions [42]. Peroxisome proliferator-activated receptor  $\gamma$ -coactivator-1 $\alpha$  (PGC1 $\alpha$ ) regulates mitochondrial biogenesis. An induction of PGC1 $\alpha$  stimulates peroxisome proliferator-activated receptor  $\gamma$  (PPAR  $\gamma$ ) to promote mitochondrial biogenesis in adipose and muscle

tissues [43]. Mitochondrial biogenesis is controlled both by mitochondrial sirtuins (such as SIRT3) and nuclear sirtuins (such as SIRT1) [44]. PGC1 $\alpha$  upregulates SIRT3 through several mechanisms [45], and may itself be upregulated through SIRT3 [46].

We used a transgenic mouse model expressing a mutated uracil-DNA glycosylase 1 (mutUNG1) enzyme, which induces mitochondrial toxicity, caused by increasingly high numbers of apyrimidinic (AP)-sites in mtDNA of fore-brain neurons [47]. AP-sites are a threat to cellular viability and genomic integrity [48, 49]. The resulting progressive mtDNA cytotoxicity leads to neurodegeneration and apoptosis [47]. Hippocampal neurons are highly sensitive to elevated levels of AP-sites in mtDNA [50]. There is a loss of the mtDNA copy number in the hippocampus of mutUNG1-expressing mice and a reduction of total mtDNA expression compared to wild type littermates [50]. A gradual elevation of the endogenous antioxidant enzyme, superoxide dismutase, has also been noticed in mutUNG1-expressing mice, indicating increased levels of ROS produced by dysfunctional mitochondria, since the mitochondrial version of superoxide dismutase (Sod2) is early and highly expressed [50]. The increased level of ROS can cause neuronal suicide [51, 52]. Thus an increasing level of AP-sites in mtDNA could be a factor that accelerates brain aging and neurodegeneration. Collectively, the mutUNG1-expressing mouse is a model for progressive neurodegeneration in the hippocampus, relating to mitochondrial dysfunction [47]. Previously, we showed that a KD increases mitochondrial mass and levels of proteins mediating electron transport (nuclear DNA encoded complex II), antioxidative defense (SOD2), mitochondrial fission (FIS1), and a longevity-associated deacetylase (SIRT1) in mutUNG1-expressing mice [53]. However, a KD nevertheless accelerates neurodegeneration in these mice, apparently because in the mutUNG1 mice the KD induced mitochondriogenesis results in only sick mitochondria [53].

In the present study, we test the effects of a KD or the ketone body  $\beta$ HB on induced mitochondrial toxicity in hippocampal tissue *in vivo* and in cells cultured *in vitro*, to explore mechanisms underlying ketone increased mitochondrial biogenesis and functions in neurological disease. We show that both a KD and  $\beta$ HB change the expression of mRNAs and proteins (UCP2, PGC1 $\alpha$ , Drp1 and Mfn1) involved in mitochondrial dynamics and biogenesis. We further find that  $\beta$ HB can rescue impaired mitochondrial respiration. Interestingly, the density of UCP2 increases in the mitochondria of neuronal somas and axon terminals, indicating a neuroprotective function of UCP2 in mutUNG1-expressing mice fed on a KD. The level of UCP2 is upregulated with a KD and  $\beta$ HB, in the hippocampus of mutUNG1-expressing mice and in cultured rat hippocampal neurons as well as cultured human

fibroblasts treated with hydrogen peroxide, respectively. Taken together, we propose that the PGC1 $\alpha$ -SIRT3-UCP2 axis is activated by KD or  $\beta$ HB treatments to rescue mitochondrial function.

## Materials and Methods

### Experimental Mice and Treatment

In this study we used transgenic mice expressing a mutated form of mitochondrial DNA repair enzyme UNG1 (mutUNG1) as previously described [47]. The expression of mutUNG1 was induced by adding doxycycline to the diet. Wild type (WT) and mutUNG1-transgenic mice were fed with standard diet (SD) for 8 weeks. After 8 weeks, mutUNG1 expression was started by feeding the transgenic mice with doxycycline mixed SD up to 4–6 months of age until death, while WT mice were continued with SD. In other mutUNG1 transgenic mice, doxycycline was added with high fat ketogenic diet (KD) (Testdiet®, St. Louis). Feeding regime was continuous. The weight of mice was monitored weekly. The mice, expressing mutUNG1 selectively in forebrain neurons, showed stable body weight for up to the observed 17 weeks on KD, but unlike mutUNG1 expressing mice on a standard diet, failed to increase in weight during the first 7 weeks ([53] Suppl Fig. 1). The mice thus were apparently in good physical condition and showed no overt behavioral phenotype during the 17 weeks. The energy content of SD and KD was described previously [53]. All experiments were approved by the National Animal Research Authority in Norway and conducted according to the laws and regulation on animal welfare in Norway and in the European Union.

### Cell Culture and Treatment

The rat hippocampal neurons (Lonza; Cat R-HI-501) were seeded onto poly-D-lysine/laminin-coated culture plates in neurobasal medium (ThermoFisher Scientific) supplemented with antibiotic–antimycotic (ThermoFisher Scientific), N21-Max media supplement (R&D Systems) and L-glutamine (Sigma-Aldrich). The  $\beta$ -hydroxybutyrate ( $\beta$ HB) treatment experiment was conducted on cell culture day 9. The rat hippocampal neurons were treated with  $\beta$ HB (7 mM) for 24 h for Western blotting analysis and NAD<sup>+</sup>/NADH ratio measurements. The human fibroblast cell lines were grown in Dulbecco's Modified Eagle Medium (DMEM, ThermoFisher Scientific) supplemented with 10% (v/v) fetal bovine serum, 2  $\mu$ M L-glutamine, penicillin and streptomycin (all from Sigma-Aldrich, St. Louis, USA). Cells were grown at 37 °C in

a humidified atmosphere of 5% CO<sub>2</sub>. The fibroblasts were treated separately and together with  $\beta$ HB (7 mM) and hydrogen peroxide (H<sub>2</sub>O<sub>2</sub>; 50  $\mu$ M) for 48 and 72 h. Cells were treated both 48 and 72 h for mitochondrial bioenergetics analysis and based on obtained results from mitochondrial respiration, cells were treated for 48 h for Western blotting analysis.

### Quantitative Real-Time Reverse Transcription PCR

Expressions of different gene markers were analyzed using quantitative real-time PCR (qRT-PCR, Applied Biosystems StepOne Plus). The PCR primers were designed by using the CLC Main Workbench 6.9.1 and synthesized by Eurofins Genomics. Each primer pair was tested for efficiency followed by checking respective melting curve. Total RNA was isolated from hippocampus of experimental mice using TRIzol reagents (Ambion, Ref. 15,596,026) followed by DNase Treatment (Qiagen) according to the manufacturer's guidelines. The concentration of RNA was measured using Nanodrop. cDNA was synthesized from isolated RNA using a High Capacity cDNA Reverse Transcription Kit (Applied Biosystem).

List of primer pairs used:

PGC1 $\alpha$ , 5'-TGTCACCACCGAAATCCT-3' and 5'-CCTGGGGACCTTGATCTT-3';

UCP2, 5'-TCCCAATGTTGCCCGTAA-3' and 5'-AAGGCAGAAGTGAAGTGG-3';

Drp1, 5'-GCCCCGTGACAAATGAAAT-3' and 5'-CAGGCATCAGCAAAGTCG-3';

Mfn1, 5'-CGAAACTTGAAGCCACTAC-3' and 5'-ACCGAAACACAATGTCCT-3';

GPR109a, 5'-GCACGCAGAATTGTGAAG-3' and 5'-GGATGGGCTGGAGAAGTAGTA-3';

$\beta$ -actin, 5'-AGATTACTGCTCTGGCTCC-3' and 5'-ATCGTACTCCTGCTTGCT-3' (reference gene).

Reverse transcription reactions were carried out in a mixture of 10  $\mu$ l Power SYBER Green PCR Master Mix (Applied Biosystem), 45 nM primer (0.2  $\mu$ l of each forward and reverse), 10 ng cDNA template (2  $\mu$ l) and nuclease free water (7.6  $\mu$ l). The qRT-PCR reactions were run on a StepOnePlus Real-Time system (Applied Biosystem) using the default settings of PCR cycling recommended by the manufacturer. The data was normalized with a reference gene,  $\beta$ -actin, and analyzed by using a standard curve method. Differences between control and treatments are assessed with Student's *t* test (*p* < 0.05).

### Tissue Preparation and Post-embedding Electron Microscopy

The procedure for tissue preparation for electron microscopy and post-embedding immunogold labeling was adapted as

described [54]. In brief, the experimental mice were anesthetized using pentobarbital (v/w, 0.3 ml/100 g). The mice were perfused transcardially with the fixative (4% formaldehyde and 0.1% glutaraldehyde in 0.1 M sodium phosphate buffer (PB)) through a peristaltic pump for 10 min after a brief flush (for a few seconds) of 2% dextran 70 in PB. The brains were dissected out and sliced in 500  $\mu\text{m}$  thickness. CA1 region was cut into small specimens (typically 0.5  $\mu\text{m}$   $\times$  0.5  $\mu\text{m}$   $\times$  1  $\mu\text{m}$ ). The specimens were cryoprotected in glycerol and freeze substituted with Lowicryl HM20 according to an electron microscopic immunogold protocol [54]. Ultrathin sections were cut (90 nm) using a diamond knife and dried at room temperature.

The hippocampal ultrathin sections on the grids were etched with 2% hydrogen peroxide ( $\text{H}_2\text{O}_2$ ) in PB droplets for 15 min. Then the tissue grids were rinsed gently in PB (3 times  $\times$  15 s). In order to neutralize free aldehyde groups in the fixed tissue, sections were treated with a solution of Tris Buffer Saline Tween (TBST) with 50 mM glycine and 0.1% sodium borohydride ( $\text{NaBH}_4$ ) droplets for 10 min and then washed in TBST. Nonspecific antibody binding sites were blocked using 2% (wt/vol) human serum albumin (HSA) in TBST solution for 10 min and followed by the same step once again. The ultrathin sections on grids were then incubated with goat anti-UCP2 primary antibody (UCP2, 1:500) overnight at 4  $^\circ\text{C}$ . They were then washed in TBST prior to being dipped in TBST droplets (10 min), followed by the same step once again. Then the grids were dipped in TBST with 2% (wt/vol) HSA droplets for 10 min. Then they were dipped in 2% HSA with polyethylene glycol (PEG) in TBST droplets (10 min) to avoid gold particle aggregation. Then the ultrathin sections on grids were incubated with rabbit anti-goat IgG secondary antibody (1:20, coupled with 10 nm colloidal gold particles in TBST with 2% HSA and PEG) for 2 h. Finally, they were rinsed with TBST followed by dipping into TBST and then rinsed in UF (ultra-filtered) water. The dried immunolabeled ultrathin sections were counterstained with 1% uranyl acetate and 0.3% lead citrate as described in the protocol [50]. Electron micrographs were taken with a FEI Tecnai 12 electron microscope at primary magnifications of  $\times 26,500$  and saved as tif files. The density of gold particles (GP) representing UCP2 was analyzed in the presynaptic terminals and somas of CA1 pyramidal neurons of the hippocampus. Density (UCP2 GP/ $\mu\text{m}^2$ ) = (Total number of UCP2 GP/ $\text{nm}^2$  total area)  $\times$  1,000,000.

### Mitochondria Isolation

Mitochondria were isolated from hippocampus of WT, SD-fed mutUNG1 and KD-fed mutUNG1 mice according to the protocol described previously [47]. In brief, mitochondria were isolated using mitochondria isolation kit (Thermo

Scientific). The isolated mitochondrial pellet was dissolved in a buffer containing 0.5% Igepal CA-630 (Sigma), 2 mM dithiothreitol (DTT), 1% protein inhibitor cocktail (Sigma) and 0.5% Triton X-100 (Sigma) in phosphate-buffered saline (PBS). Then mitochondria were incubated on ice for 5 min prior to vortex for 1 min. The mitochondrial total protein concentration was measured using Bicinchoninic acid protein assay kit (Pierce).

### Western Blotting

Western blotting assay was carried out using mitochondrial isolate (1 mg/ml, 20  $\mu\text{l}$ ) from mouse hippocampus from 3 different groups, human cancer associated fibroblast cells and rat hippocampal neurons treated with a ketone body ( $\beta\text{HB}$ , 7 mM) and hydrogen peroxide ( $\text{H}_2\text{O}_2$ ; 50  $\mu\text{M}$ ). The total protein concentration was measured using Direct Detect<sup>TM</sup> (Millipore). Western blotting was performed according to our previously published article [47, 53]. In brief, the proteins in SDS-PAGE gel were transferred onto a nitrocellulose membrane and incubated with primary antibody to UCP2 (Sigma-Aldrich SAB2501087 and Cell Signaling Technology, Cat. 89,326; 1:500), PGC1 $\alpha$  (Abcam ab54481; 1:1000 and Novus Biologicals, Cat. NBP1-04676SS; 1:1000), Drp1 (Abcam ab54038; 1:2000 and Cell Signaling Technology, Cat. 8570; 1:000), Mfn1 (Abcam ab104585; 1:1000), sirtuin 3 (SIRT3: Cell Signaling technology, Cat. 2627; 1:1000), cytochrome C (CytC; Cell Signaling Technology, Cat. 11,940; 1:1000) and  $\beta$ -actin (Millipore MAB1501R; 1:5000). The nitrocellulose membrane was incubated for 1 h with secondary antibody conjugated with horseradish peroxidase (HRP), for PGC1 $\alpha$ , Drp1, SIRT1, SIRT3, CytC and Mfn1 with goat anti-rabbit IgG (BIO-RAD, Cat 170–6515; 1:20,000), for UCP2 with rabbit anti-goat IgG (ThermoFisher Scientific, Cat. R-21,459; 1:20,000), and for  $\beta$ -actin with rabbit anti-mouse IgG (Sigma-Aldrich, Cat. A9044; 1:20,000). Notably, all protein targets were developed on the same membrane followed by consecutive stripping of the membrane for 30 min using stripping buffer (ThermoFisher Scientific). The protein band was visualized with a digital imaging system (Image Reader LAS-3000).

### Mitochondrial Respiration Measurements

SeaHorse Bioscience methodology was used to measure oxygen consumption rate (OCR). The human cancer associated fibroblast cells were harvested and re-suspended (the cell number was normalized to 20,000 cells/80  $\mu\text{l}$ ) to seed in 80  $\mu\text{l}$  of growth medium in an Agilent SeaHorse cell culture 96-well microplate. The culture plates were incubated overnight and the cells were treated with  $\beta$ -hydroxybutyrate ( $\beta\text{HB}$ ; 7 mM) and hydrogen peroxide

(H<sub>2</sub>O<sub>2</sub>; 50 μM). Cell growth was monitored before the treatment using a microscope. Cells were treated for 48 and 72 h. The sensor cartridge was hydrated with SeaHorse Bioscience XF96 calibrant overnight in the Prep Station (37 °C, w/o CO<sub>2</sub>) before running the cell culture microplate. Test assay medium was prepared by adding 2 mM L-glutamine (Life Technologies, 25030-081), 10 mM glucose (Sigma, G7528), 5 mM pyruvate (Sigma, S8636) into XF Base Medium (Agilent Technologies, Cat. 102353-100). Cells were washed using pre-prepared assay medium according to the instructions by SeaHorse Bioscience. Then culture microplate was placed in a 37 °C incubator without CO<sub>2</sub> for an hour prior to the assay. The Sensor Cartridge was prepared by adding 25 μl of assay medium to port A with 3 μM oligomycin (Sigma, 495,455), to port B with 2 μM CCCP (Sigma, C2579), to port C with 1 μM rotenone (Sigma, R8875), and to port D with 1 μM antimycin A (Sigma, A8674). After the run was completed, the cell microplate was washed with PBS, transferred to a -80 °C freezer and left overnight. The protein concentration was determined for each well in the microplate using a BCA protein assay (ThermoFisher Scientific), and used to normalize the SeaHorse XF96 primary data.

### NAD<sup>+</sup>/NADH Ratio Measurements

The NAD<sup>+</sup>/NADH ratio is an essential parameter for mitochondrial function. We measured the NAD<sup>+</sup>/NADH ratio using NAD<sup>+</sup>/NADH-Glo™ bioluminescent assay (Promega) as described previously [55]. In brief, rat hippocampal neurons (Lonza; Cat R-HI-501) were treated with β-hydroxybutyrate (βHB; 7 mM) and/or hydrogen peroxide (H<sub>2</sub>O<sub>2</sub>; 50 μM) for 24 h. Cell lysates were collected from each sample groups. Then each sample was divided into two parts separately for NAD<sup>+</sup> and NADH measurement. To measure NAD<sup>+</sup>, one part of sample was treated with 0.4 N HCl followed by adding Trizma base (Sigma-Aldrich) and the other part of sample was treated with Trizma® base to quantify NADH. In each step, samples were heated at 60 °C for 15 min before treating with Trizma base. The luminescence from HCl and Trizma® base-treated samples represented the amount of NAD<sup>+</sup> and NADH, respectively.

### Statistical Analysis

Quantification of EM data of candidate protein, UCP2, in various subcellular areas (presynaptic terminals and somas) were assessed using a two-tailed Student's *t* test where *p* < 0.05 is defined as significant. The same was applied for showing quantitative differences of genes

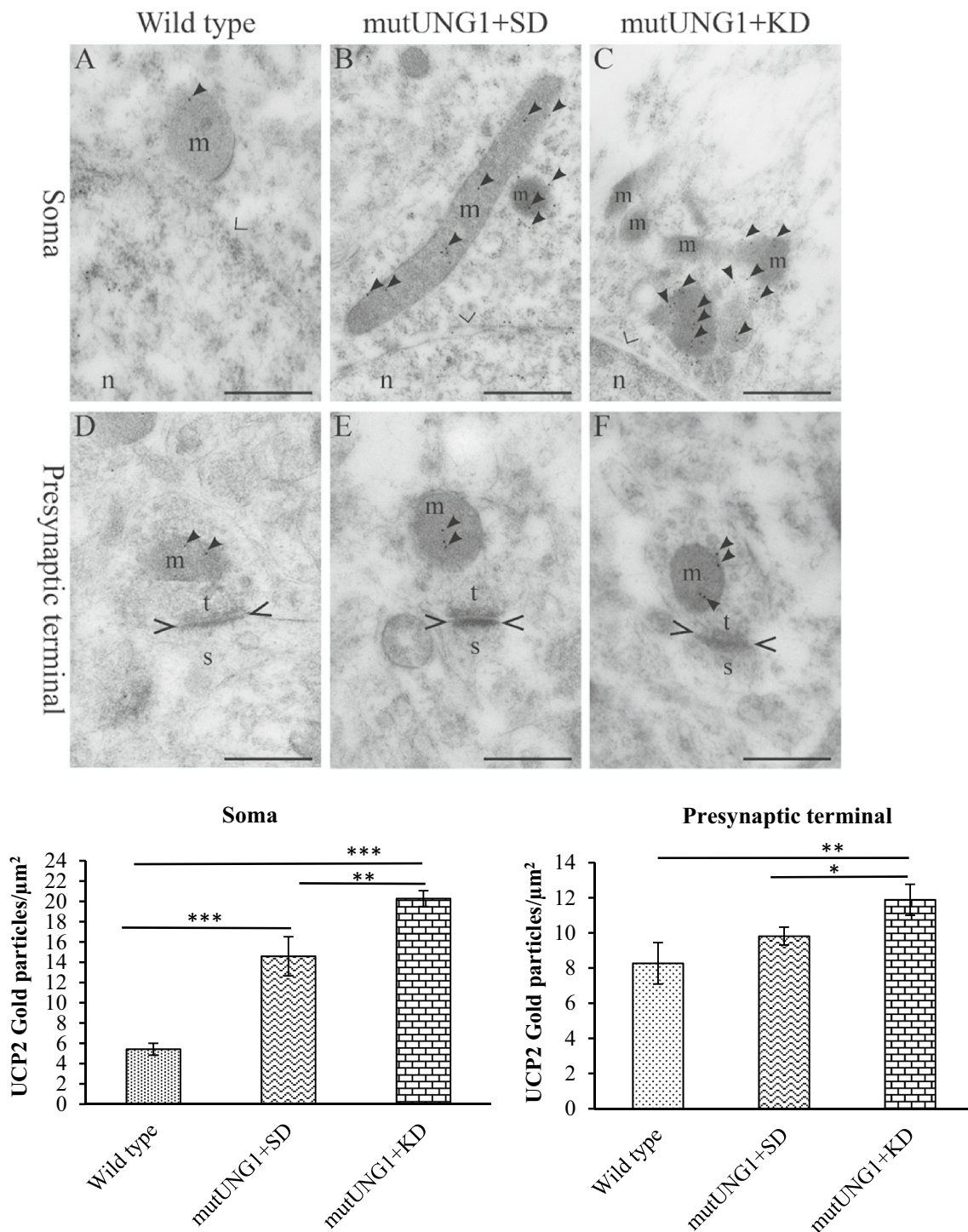
and proteins expression between different experimental groups. The level of significance is symbolized with \* (*p* value ≤ 0.05), \*\* (*p* value ≤ 0.01), and \*\*\* (*p* value ≤ 0.001). The statistical analysis was performed using Microsoft Excel 2010. The quantitative differences of OCR and NAD<sup>+</sup>/NADH ratio among groups were assessed with a one-way ANOVA test using SPSS, where *p* < 0.05 is defined as significant (Tukey tests, *p* < 0.05). Data are presented as mean ± SE or mean ± standard deviation (*n* = 3 mice), as stated.

## Results

### A Ketogenic Diet Elevates the level of UCP2 in Mitochondria of Neuronal Perikarya and Nerve Endings and Changes Mitochondrial Morphology in the Hippocampus of Mice During mutUNG1 Induced Oxidative Stress

Ketogenic diet increases mitochondrial mass in a mouse model in which an induced mutated version of UNG1 (mutUNG1) causes mitochondrial dysfunction [53]. Prompted by the apparent upregulation of the mitochondrial antioxidant system in mice expressing mutUNG1 [53] we examined the subcellular levels of the mitochondrial proton and anion carrier protein, UCP2, which uncouples oxidative phosphorylation by a leak current reducing the membrane potential that drives ATP production and thereby curbs the generation of ROS [30]. Through post-embedding immunogold labeling, mitochondrial UCP2 was found to be present in mitochondria of CA1 pyramidal cell bodies, and in nerve terminal in stratum radiatum, in both WT littermates and mutUNG1-expressing mice (Fig. 1). In the WT fed SD, the UCP2 density was higher in the terminals than in the somas. The density of UCP2 in somas and in axon terminals was raised significantly in mutUNG1-expressing mice fed a KD compared to mutUNG1-expressing mice (or WT littermates) fed a SD (Fig. 1).

The mutUNG1-expressing mice showed a wide variety of mitochondrial shapes in the somas, as previously reported [53]. The shape of mitochondria was not much varied in presynaptic terminals (Fig. 1d–f), while somas of mutUNG1-expressing mice showed aggregated, clustered, and irregularly shaped mitochondria and an increase in the total mitochondrial volume, the changes being larger in mice fed a KD (Fig. 1b, c; and reference [53]). Clusters or aggregates of mitochondria may represent fusion and/or fragmentation, more in somas due to retrograde transport of the mitochondria to somas to get repaired [56]. WT mice showed a regular structure of mitochondria in somas and terminals (Fig. 1a, d).



**$\beta$ -Hydroxybutyrate Restores Mitochondrial Activity from Impairment by  $\text{H}_2\text{O}_2$  Induced Oxidative Stress**

The human cancer associated fibroblast cell line was cultured to measure the real-time mitochondrial respiration in an extracellular flux analyzer (SeaHorse Biosciences). The analyzer measured the mitochondrial OCR in a transient microchamber over 3 min representing mitochondrial

respiration. The mitochondrial OCR was significantly increased in  $\beta\text{HB}$  (7 mM) treated cells (48 h:  $52.97 \pm 0.50$ ; 72 h:  $50.85 \pm 0.49$  pmol/min) compared to control cells (48 h:  $47.80 \pm 1.21$ ; 72 h:  $45.55 \pm 1.07$  pmol/min) (mean  $\pm$  standard deviation,  $n=3$  replicate wells) for both 48 and 72 h stimulation (48 h:  $p=0.002$ ; 72 h:  $p=0.000$ ) (Fig. 2a, b). Importantly, cells treated with  $\text{H}_2\text{O}_2$  (50  $\mu\text{M}$ ) to induce OS showed a reduced OCR (48 h:  $36 \pm 1.09$ ;

**Fig. 1** A ketogenic diet increases the level of UCP2 in the CA1 pyramidal cell somas and axon terminals of mutUNG1-expressing mice. Electron microscopic immunogold localization of mitochondrial UCP2 **a–c** at the CA1 pyramidal cell somas and **d–f** at the presynaptic terminals in the CA1 stratum radiatum of WT (**a** and **d**), mutUNG1-expressing mice fed a standard diet (SD) (mutUNG1+SD) (**b** and **e**) and mutUNG1-expressing mice fed a ketogenic diet (KD) (mutUNG1+KD) (**c** and **f**). Below: Immunogold quantification of UCP2 density (UCP2 gold particles/ $\mu\text{m}^2$ ) at the CA1 pyramidal cell somas and at the presynaptic terminal of hippocampus CA1. The density of UCP2 was statistically significantly elevated in mutUNG1+KD mice compared to mutUNG1+SD mice, in somas as well as terminals. The increased level of UCP2 in the somas of mutUNG1-expressing compared to WT mice paralleled the concomitant increase of mitochondrial dysfunction. Data represent average values from 20 to 30 electron micrographs (EMs) containing 45–63 EM profiles for the somas and for the presynaptic terminals from each mouse, and are presented as mean  $\pm$  SE ( $n=3$ , number of mice from each group). The level of significance is symbolized with \* ( $p$  value  $\leq 0.05$ ), \*\* ( $p$  value  $\leq 0.01$ ), and \*\*\* ( $p$  value  $\leq 0.001$ ). Black arrowheads = gold particles representing UCP2, *m* mitochondria, *t* presynaptic terminal, *s* dendritic spine, and *n* nucleus. The nuclear membrane (thin V) and post synaptic density (thick V) are indicated. Scale bar: 500 nm

72 h:  $28.78 \pm 0.73$  pmol/min), which was significantly restored by co-treatment with  $\beta$ HB in addition to  $\text{H}_2\text{O}_2$  (48 h:  $42.53 \pm 1.33$ ; 72 h:  $35.03 \pm 0.99$  pmol/min) for both 48 and 72 h (48 h:  $p = 0.000$ ; 72 h:  $p = 0.000$ ) (Fig. 2a, b). There was a statistically significant (48 h:  $p = 0.002$ ; 72 h:  $p = 0.000$ ) increment of OCR in cells treated with  $\beta$ HB (48 h:  $52.97 \pm 0.50$ ; 72 h:  $50.85 \pm 0.49$  pmol/min) compared to co-treatments with  $\beta$ HB and  $\text{H}_2\text{O}_2$  (48 h:  $42.53 \pm 1.33$ ; 72 h:  $35.03 \pm 0.99$  pmol/min) (Fig. 2a, b). The  $\text{NAD}^+/\text{NADH}$  ratio was measured in rat hippocampal neurons treated with  $\beta$ HB (7 mM) and  $\text{H}_2\text{O}_2$  (50  $\mu\text{M}$ ). Similarly to the findings on OCR in human fibroblasts,  $\text{H}_2\text{O}_2$  significantly decreased the  $\text{NAD}^+/\text{NADH}$  ratio in the neurons, while  $\beta$ HB significantly increased the ratio in controls and rescued the decrease caused by  $\text{H}_2\text{O}_2$  (Fig. 2c).

### A Ketogenic Diet and $\beta$ -Hydroxybutyrate Both Increase the Levels of Proteins Involved in Mitochondrial Biogenesis, Uncoupling, Fission and Fusion

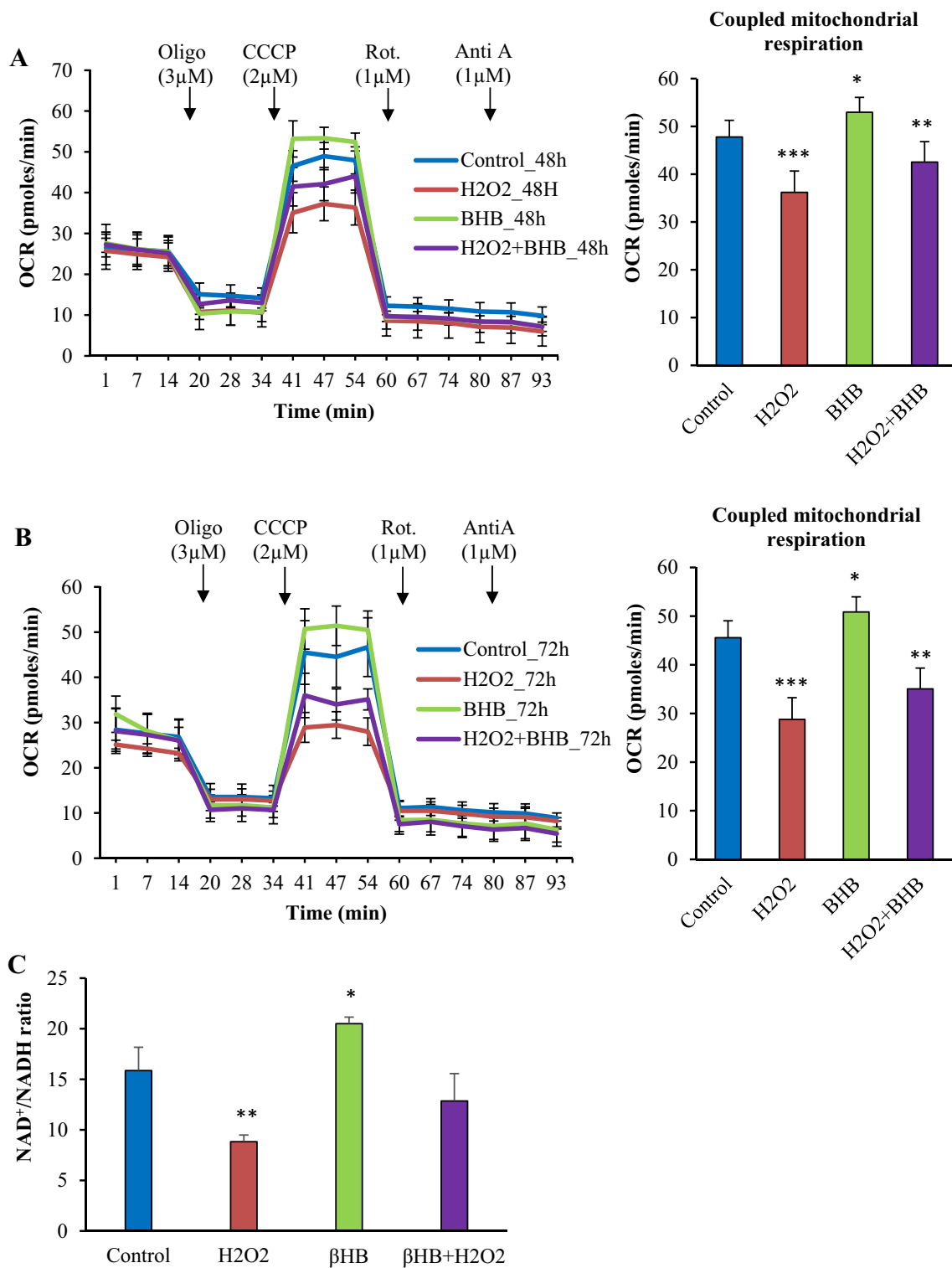
In line with the reported breakdown of mitochondrial function in mutUNG1-expressing mice [49], we investigated the levels of proteins controlling mitochondrial key functions, i.e., biogenesis, uncoupling, fission and fusion. We explored the proteins in rat hippocampal neurons and human fibroblasts treated with  $\beta$ HB (7 mM, 24 h and 48 h respectively), after being challenged with  $\text{H}_2\text{O}_2$  treatment (50  $\mu\text{M}$ , 48 h), and in hippocampi of mutUNG1 mice on a KD [53]. Western blotting analysis showed that there was a significant increase of PGC1 $\alpha$  protein, the ‘master regulator’ of

mitochondrial biogenesis, in mutUNG1-expressing mice fed a KD ( $p < 0.008$ ) compared to the model mice fed a SD (Fig. 3a). Furthermore, PGC1 $\alpha$  protein content was decreased in human fibroblasts and in rat hippocampal neurons treated with  $\text{H}_2\text{O}_2$ , a pharmacological way to induce OS and damage mitochondrial function in vitro, and the decrease was rescued by co-treatment with  $\beta$ HB and  $\text{H}_2\text{O}_2$  (Fig. 3b, c).

An increased level of mitochondrial UCP2 has previously been reported to be involved in mitochondrial biogenesis [57]. The level of UCP2 was increased in mutUNG1-mice fed a SD, compared to WT fed a SD, and further raised in the transgenic model mice fed a KD (Fig. 3a). The tendency to increased level of UCP2 in response to KD did not reach statistical significance, but was supported by in vitro experiments, which suggested that  $\beta$ HB could reverse the reduction of UCP2 by  $\text{H}_2\text{O}_2$  treatment (Fig. 3b). As expected,  $\beta$ HB treatment showed the ability to increase the level of UCP2 in hippocampal neurons and the level of UCP2 followed the same expression pattern with  $\text{H}_2\text{O}_2$  and  $\beta$ HB treatments (Fig. 3c). We investigated key proteins controlling mitochondrial fusion, such as mitofusion 1 (Mfn1), and dynamin-related protein 1 (Drp1), which mediates fission dynamics. A significant increase of Drp1 expression was found in mutUNG1-expressing mice fed a KD compared to WT littermates on SD ( $p < 0.013$ ) (Fig. 3a), which might shift more mitochondria towards fission in response to a KD diet. The same tendency was also noticed when fibroblast and hippocampal neuronal cells were treated with  $\text{H}_2\text{O}_2$  and  $\beta$ HB elevated the level of Drp1 (Fig. 3b, c). We further investigated the expression of SIRT3, a mitochondrial  $\text{NAD}^+$  dependent deacetylase, and found that  $\beta$ HB could elevate the level of SIRT3 lowered by  $\text{H}_2\text{O}_2$  (Fig. 3b, c). The  $\text{H}_2\text{O}_2$  induced OS [58], reveals itself by an increased level of the mitochondrial marker CytC (released through the mitochondrial permeability transition pore causing apoptosis), which was reduced by  $\beta$ HB (Fig. 3b).

### Expression of Genes Involved in Mitochondrial Biogenesis, Uncoupling, Fission and fusion were Altered in the Hippocampus of Ketogenic Diet Fed mutUNG1-expressing Mice

We further investigated the expression of pivotal genes for mitochondrial biogenesis, uncoupling, fission and fusion using qRT-PCR. The effects of KD on mRNA levels were generally clearer than those on the protein levels. PGC1 $\alpha$  mRNA was reduced in mutUNG1-expressing mice compared to WT fed a SD, but was significantly upregulated in response to KD in mutUNG1-expressing mice ( $p < 0.05$ ) (Fig. 4a). The level of UCP2 mRNA was significantly higher in KD-fed mutUNG1-expressing mice compared to both



WT littermates ( $p < 0.01$ ) and mutUNG1-mice fed a SD ( $p < 0.04$ ) (Fig. 4b). Equilibrium between fusion and fission controls the morphology of the mitochondria [59] and the physiological function of neurons [60]. Genes associated with fission (Drp1) (Fig. 4c) showed a significant upregulation in mutUNG1-expressing mice fed a KD compared

with WT littermates ( $p < 0.05$ ). A significant downregulation of the mitochondrial fusion gene, Mfn1, was found in KD-fed compared to SD-fed mutUNG1-expressing mice ( $p < 0.02$ ) (Fig. 4d). An alteration of both fusion and fission in mutUNG1-expressing mice may have aggravated mitochondrial dysfunction on a KD.

**Fig. 2** A ketone body ( $\beta$ HB) improves mitochondrial bioenergetics. The oxygen consumption rate (OCR) was measured using extracellular flux analysis (SeaHorse XF96) on monolayers of human cancer associated fibroblast cells treated with the ketone body  $\beta$ -hydroxybutyrate ( $\beta$ HB) (7 mM), with and without induction of OS by hydrogen peroxide ( $\text{H}_2\text{O}_2$ ; 50  $\mu\text{M}$ ) for **a** 48 and **b** 72 h. Subsequently, ATP synthase inhibitor (oligomycin; Oligo), mitochondrial uncoupler (ionophore carbonyl cyanide *m*-chlorophenylhydrazone; CCCP), complex I inhibitor (rotenone; Rot.), and complex III inhibitor (antimycin A; AntiA) were added in order to determine the effects of  $\beta$ HB on mitochondrial respiration. Mitochondrial coupled respiration was significantly decreased by the treatment with  $\text{H}_2\text{O}_2$ . The reduction was partly reversed by  $\beta$ HB at both 48 and 72 h.  $\beta$ HB treated cells showed a higher respiratory capacity than control cells. Furthermore, we observed a striking increase in the respiratory capacity with  $\beta$ HB treated cells after the addition of CCCP. **c** Rat hippocampal neurons treated with  $\beta$ HB (7 mM; 24 h) for  $\text{NAD}^+/\text{NADH}$  ratio measurements ( $n=3$  separate culture samples) and shows significant alteration of  $\text{NAD}^+/\text{NADH}$  ratio by  $\beta$ HB and  $\text{H}_2\text{O}_2$  treatments. Statistics indicated as in Fig. 1. The quantitative differences among groups were assessed with one-way ANOVA test (post hoc Tukey tests,  $p < 0.05$ ). (Color figure online)

We then explored whether a KD regulated the ketone body  $\beta$ HB receptor, GPR109a (also known as HCAR2), and interestingly found that the level of expression was significantly elevated on a KD in mutUNG1-expressing mice compared to both WT ( $p < 0.04$ ) and mutUNG1-expressing mice fed a SD ( $p < 0.05$ ) (Fig. 4e). We further examined the expression level of lactate receptor, GPR81 (also known as HCAR1), which has high sequence and structural similarity with GPR109a [61]. GPR81 contrasts with GPR109a by being reduced in mutUNG1 compared with WT, and by not being significantly upregulated by KD, i.e., attesting to a selective influence of KD on the ketone body receptor (Fig. 4f).

## Discussion

### Ketogenic Diet and $\beta$ -Hydroxybutyrate Increase the Expression of the Mitochondrial Uncoupling Protein UCP2

While in the WT UCP2 labeling density is higher in the axon terminals than in pyramidal cell somas in hippocampus CA1, the mutUNG1-expressing mice showed higher UCP2 labeling in the pyramidal cell somas (Fig. 1). The mutUNG1-expressing mice exhibit a significantly higher density of UCP2 in the somas after KD compared to SD (Fig. 1). A somewhat lesser effect occurred in the synaptic terminals. Our data indicate that an increased mass of dysfunctional and unhealthy mitochondria produced by mutUNG1-expressing mice have followed the mitochondrial retrograde transport and accumulated in the somas to get repaired or disposed of, making it possible to supply

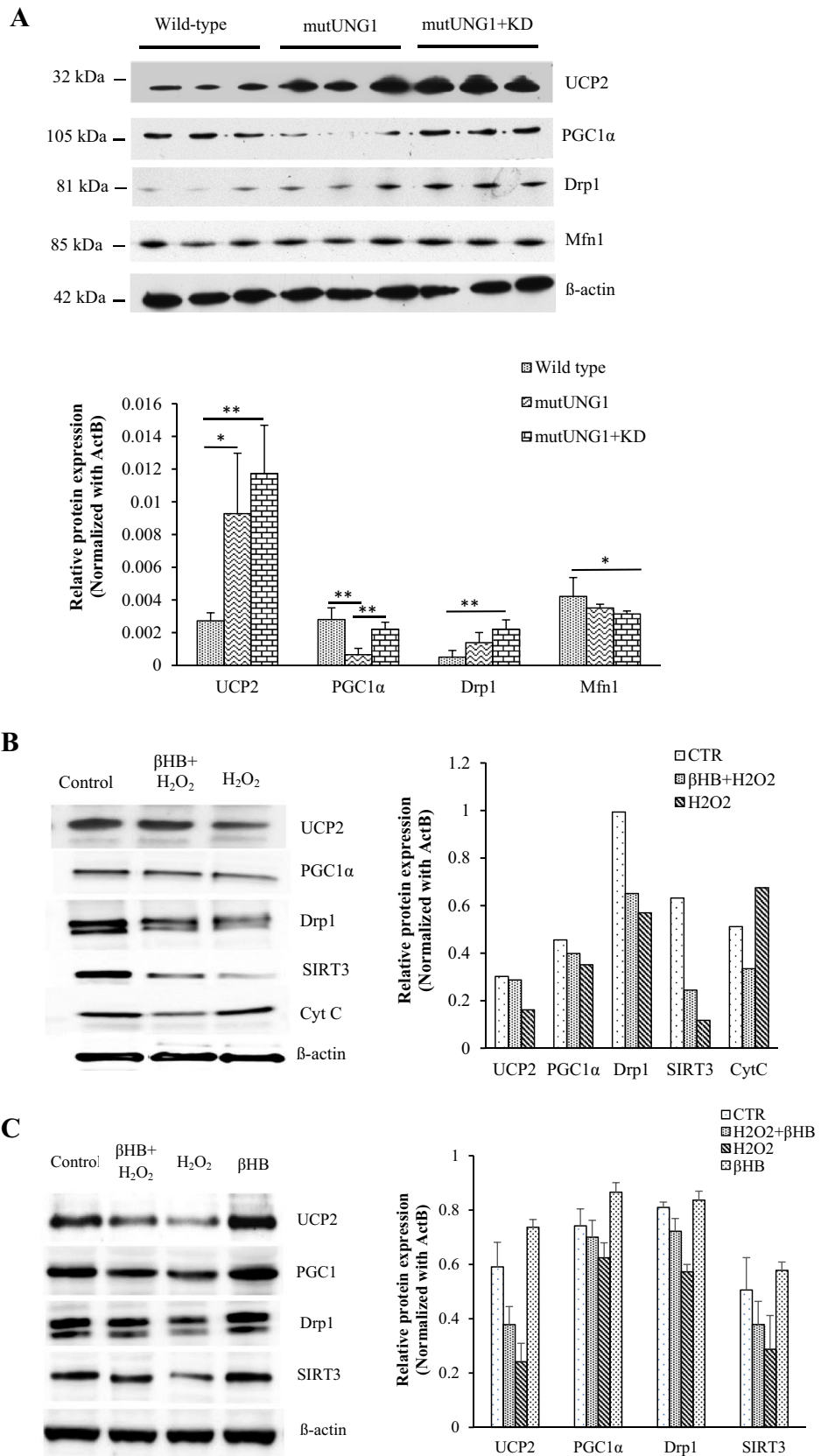
healthy mitochondria to the synaptic terminal/distal parts of the neurons and get neuroprotection [62], and that this process is enhanced by a KD. To our knowledge we are the first to analyze UCP2 at the subcellular level in neurons, and to show changes in UCP2 distribution in a model of mitochondrial dysfunction.

The present study is consistent with studies in other neurodegenerative models that support the role of UCP2 as a neuroprotective against neuropathologies [62, 63]. The role of UCP2 in counteracting OS and ROS generation in the brain is well-described [62]. We also find that signs of dysfunctional mitochondria in terms of altered mitochondrial shape and fragmentation are present more often in the somas of CA1 pyramidal neurons in mutUNG1-expressing mice fed a KD (Fig. 1c) compared to SD (Fig. 1b). The present study is consistent with previous reports that dysfunctional mitochondria are fragmented and accumulated in neuronal somas in Huntington's disease [56]. A KD increases the number of mitochondria in the brain and in muscle cells [38, 64–66]. Our findings however, indicate that aged and dysfunctional mitochondria might get protection from UCP2 in the somas and thereby promote supply of healthy mitochondria to the distal parts of neurons. The KD enhanced levels of UCP2 in the pyramidal cell soma in the mutUNG1-expressing mice suggests that more ROS might be produced in the mitochondria of cell somas, manifested by higher level of endogenous antioxidant [50] and more mitochondrial fragmentation and aggregation [53] in mutUNG1-expressing mice. This increased mitochondrial fragmentation and aggregation (Fig. 1c) might relate to the higher quantity of UCP2 in somas of mutUNG1-expressing mice compared to WT littermates (Fig. 1a). Neurons are highly specialized cells that face unique challenges, such as requiring large amounts of energy for neuronal communication. A defect in mitochondrial function is a key feature in neurodegenerative diseases and aging. Aggregation of mitochondria in the soma is also a common step preceding apoptosis [60]. The level of UCP2 decreased in  $\text{H}_2\text{O}_2$ -exposed fibroblasts while  $\beta$ HB helped to elevate it (Fig. 3b), suggesting a protective role of UCP2 against OS. Attesting to the importance of this, UCP2 plays a key role in protecting mice from aging [34].

### $\beta$ -Hydroxybutyrate Restores Mitochondrial Respiration and Activity from Damage by Oxidative Stress

$\beta$ HB is a metabolic intermediate, synthesized by hepatocytes from acetyl-CoA, that is utilized as an alternative energy source.  $\beta$ HB oxidation has been reported to be associated with high nicotinamide adenine dinucleotide (NADH) production, and increases the

**Fig. 3** A ketogenic diet and a ketone body ( $\beta$ HB) increase proteins that regulate mitochondrial biogenesis. Western blotting assay was performed on protein from **a** mouse total hippocampal extract (20  $\mu$ g) and **b** human cancer associated fibroblast cells lysate (20  $\mu$ g). The fibroblasts were treated with  $\beta$ -hydroxybutyrate ( $\beta$ HB; 7 mM) and hydrogen peroxide ( $H_2O_2$ ; 50  $\mu$ M) for 48 h. **a** The tissue levels of the proteins UCP2, biogenesis regulator PGC1 $\alpha$  and dynamin-related protein Drp1 were increased in the hippocampus of mutUNG1-expressing mice fed a ketogenic diet (KD). Data are expressed as mean  $\pm$  standard deviation (n = 3 mice in each group). Statistical significance levels are indicated as in Fig. 1. **b** The in vitro effects of  $H_2O_2$  induced OS in human fibroblasts mimicked, in part, the mitochondrial dysfunction in mutUNG1 expressing mice, leading to reduced expression of the mitochondrial key proteins PGC1 $\alpha$ , Drp1, and SIRT3, which was partly rescued by  $\beta$ HB. **c** Rat hippocampal neurons treated with  $\beta$ HB (7 mM) and  $H_2O_2$  (50  $\mu$ M) for 24 h (data presented as mean  $\pm$  SD, n = 2 repeated experiments). The  $\beta$ HB tended to elevate the levels of UCP2, PGC $\alpha$ , SIRT3 and DRP1 while the opposite occurred by  $H_2O_2$  treatment, which was rescued by  $\beta$ HB



phosphorylation potential in canine heart in vivo [67].  $\beta$ HB can rescue dopaminergic neuronal degeneration induced by 1,2,3,6-tetrahydropyridine (MPTP) in mice [68]. Moreover,  $\beta$ HB treatment facilitates B-cell survival and mitochondrial respiration [69]. Herein, we show that  $\beta$ HB protects human fibroblasts from OS induced by  $H_2O_2$  exposure (Fig. 2a, b). The rate of OCR decreased with  $H_2O_2$  exposure while co-treatment with  $\beta$ HB rescued mitochondrial respiration (Fig. 2a, b). Thus, the present study reveals that the ketone body,  $\beta$ HB, confers protection against pharmacological damage of mitochondrial respiration induced by  $H_2O_2$ . Mitochondrial respiration is required for ATP generation, and the ability of  $\beta$ HB to rescue mitochondrial OCR could help in restoring cellular metabolism. Mitochondria are the crucial source of ROS generation, and an exposure to  $H_2O_2$  leads to increased production of ROS, thereby increasing the mitochondrial OS. Importantly, our finding showed that  $\beta$ HB is protective against OS in both human fibroblasts and rat hippocampal neurons (Fig. 2a, c), which is in line with other studies showing a neuroprotective role of  $\beta$ HB [70]. An increased ratio of  $NAD^+/NADH$ , a parameter of mitochondrial function, in  $\beta$ HB-treated hippocampal neurons suggests an enhanced activity of the mitochondrial electron transport chain, as has been reported previously [55].

### **A Ketogenic Diet and $\beta$ -Hydroxybutyrate Enhance the Expression of Proteins and Genes Involved in Mitochondrial Biogenesis and Dynamics, and of the Ketone Body Receptor GPR109a**

A KD has previously been shown to increase mitochondrial mass in neuronal tissue [53], presumably through upregulation of PGC1 $\alpha$ , a master regulator of mitochondrial biogenesis demonstrated in mouse liver and brown adipose tissue [39, 71]. Here, we show that the expression level of PGC1 $\alpha$  increases in mutUNG1-expressing mice fed a KD (Fig. 3a) and in  $\beta$ HB-treated cells exposed to  $H_2O_2$  (Fig. 3b). The expression of UCP2 transcript and protein was significantly higher in mutUNG1-expressing mice fed a KD compared to SD (Figs. 3a and 4b). The elevated level of PGC1 $\alpha$  could be caused by an upregulation of UCP2 for mitochondrial uncoupling to rescue from damage by the excessive ROS, which is generated in mutUNG1-expressing mice fed a KD [50]. A co-treatment with  $\beta$ HB and  $H_2O_2$  in fibroblasts shows the beneficial effects of  $\beta$ HB to rescue cells from OS damage. This may include enhancing fission dynamics through upregulating Drp1 (Figs. 3a, b and 4c). Mitochondria are dynamic organelles that constantly divide and fuse, thus forming interconnected networks or fragmented units within the cell [60, 72, 73]. Equilibrium between fusion and fission

controls the morphology of the mitochondria [59]. We investigated key proteins regulating mitochondrial fusion and fission dynamics. A KD increased the expression of Drp1 (Figs. 3a, b and 4c), a key regulator of mitochondrial fission. An elevated level of Drp1 on a KD and on  $\beta$ HB-treatment implies enhancement of the frequency of fission, serving to protect from mitochondrial toxicity. Sirtuin 3 (SIRT3), a mitochondrial  $NAD^+$ -dependent deacetylase, is an important activator for oxidative phosphorylation [74] and lack of its expression induces decreased mitochondrial biogenesis [14]. A study suggests that mice lacking the SIRT3 gene are unable to keep normal levels of ketone bodies upon fasting [75], and ketone bodies ( $\beta$ HB and acetoacetate) protect mice against ischemic stroke following transient middle cerebral artery occlusion by upregulating the expression of brain SIRT3 [41]. SIRT3 rescues hepatocytes from oxidative damage [76]. SIRT3 plays a key role in mitochondrial function through the PGC1 $\alpha$ -SOD2 mediated pathway [77]. We show that  $\beta$ HB increases the level of SIRT3 in  $H_2O_2$ -treated fibroblasts (Fig. 3b), which suggests a protective role of  $\beta$ HB through activation of SIRT3. The monocarboxylate transporters (MCTs) are required for a ketone body to cross the BBB [23], and MCT1 and  $\beta$ HB transport are upregulated by a KD [24]. Here, we show that  $\beta$ HB upregulates the expression level of the  $\beta$ HB receptor, GPR109a (Fig. 4e), suggesting a regulatory role of  $\beta$ HB for its receptor and transporters. Further investigations are required to explore the role of GPR109a activation for the effects of KD and  $\beta$ HB on mitochondrial function.

UCP2-SIRT3 signaling has been reported to decrease mitochondrial OS [46]. In line with the proposed role of UCP2 in improving the  $NAD^+/NADH$  ratio [46], we show that a KD increases the level of UCP2, which supports the findings that a high fat diet increases the  $NAD^+/NADH$  ratio [78]. An elevated level of  $NAD^+/NADH$  ratio in  $\beta$ HB-treated hippocampal neurons supports the effects of  $\beta$ HB in increasing level UCP2-PGC1 $\alpha$  and SIRT3 (Fig. 2c). It has also been assumed that the increased level  $NAD^+/NADH$  ratio could modulate SIRT3 and PGC1 $\alpha$  to elevate mitochondrial biogenesis during cerebral ischemia–reperfusion injury [46]. To our knowledge, we are the first to show experimentally that a KD or a ketone body activates the PGC1 $\alpha$ -SIRT3-UCP2 pathway in OS conditions.

A simplified scheme of the actions of KD and ketone bodies on brain mitochondria is presented in Fig. 5. Due to the complex network of interactions, the open arrows do not represent a simple sequence of events. The studies in live mice and cultured cells concur to show that ketones ameliorate the deleterious effects of OS. However, in the mutUNG1 mice, the ameliorative effects are overwhelmed

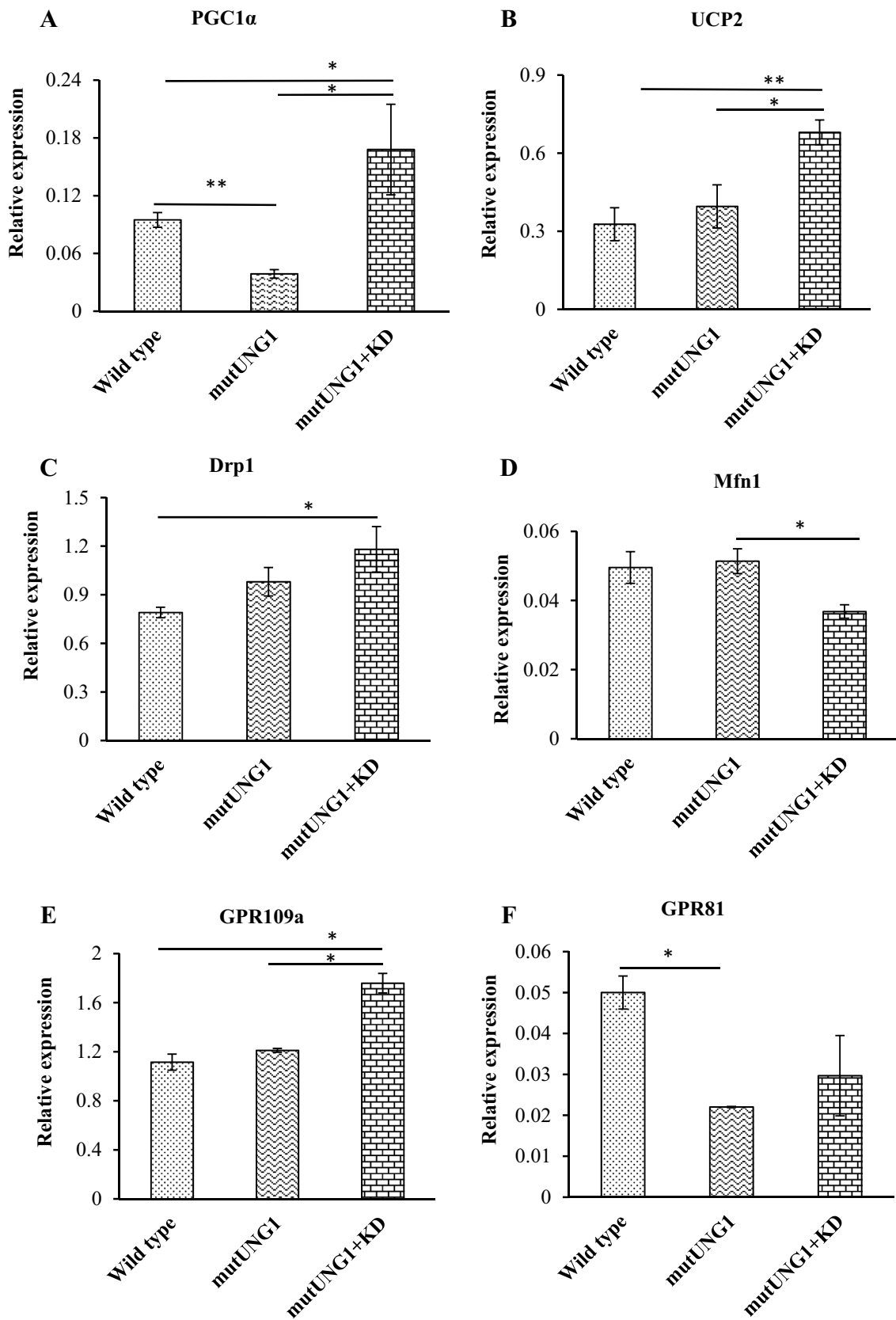


**Fig. 4** A ketogenic diet shows altered key genes expression associated with mitochondrial biogenesis, uncoupling, dynamics and its receptor activation. We investigated mRNAs encoded by genes controlling mitochondrial biogenesis (PGC1 $\alpha$ ), uncoupling (UCP2), fission (Drp1) and fusion (Mfn1) in hippocampal tissue using quantitative real time PCR (qPCR). We also examined the expression of GPR109a, a receptor selectively stimulated by the ketone body,  $\beta$ HB. Quantitative RT-PCR shows a significant downregulation of PGC1 $\alpha$  expression **a** in mutUNG1-expressing mice fed a SD compared to WT littermates and the expression level is significantly upregulated in response to a KD treatment. **b** The mitochondrial UCP2 is significantly higher in mutUNG1-expressing mice fed a KD compared to WT littermates and mutUNG1-expressing mice fed a SD. **c** The expression of Drp1, which governs mitochondrial fission, is increased in mutUNG1-expressing mice fed a KD. **d** An opposite effect is found for Mfn1. **e** The expression of the ketone body receptor, GPR109a, was significantly increased in response to a KD in mutUNG1-expressing mice. **f** The lactate receptor, GPR81, while downregulated in mutUNG1-expressing mice compared to WT, was not significantly changed in response to KD. Data are expressed as mean  $\pm$  SE (n=3). Statistical significance is indicated as in Fig. 1

(grey arrow) by the functional deficiency being propagated also in the newly formed mitochondria. Hence the increased oxidation caused by KD makes KD deleterious in these model mice [53]. Nevertheless, the mice expressing mutUNG1 (selectively in forebrain neurons) kept a constant body weight during 7 weeks on a KD [53], indicating good bodily health. They showed no overt behavioral phenotype. In future studies, it will be interesting use cognitive tests to examine whether a KD modifies OS induced behavioral deficits.

In conclusion, the results presented here suggest that a KD and  $\beta$ HB treatments help to increase mitochondrial mass and functional competence, apparently via the “PGC1 $\alpha$ -SIRT3-UCP2 axis”.

**Acknowledgements** This study was supported by research Grants from the Research Council of Norway, the Norwegian Health Association, and the Lundbeck Foundation (Denmark).

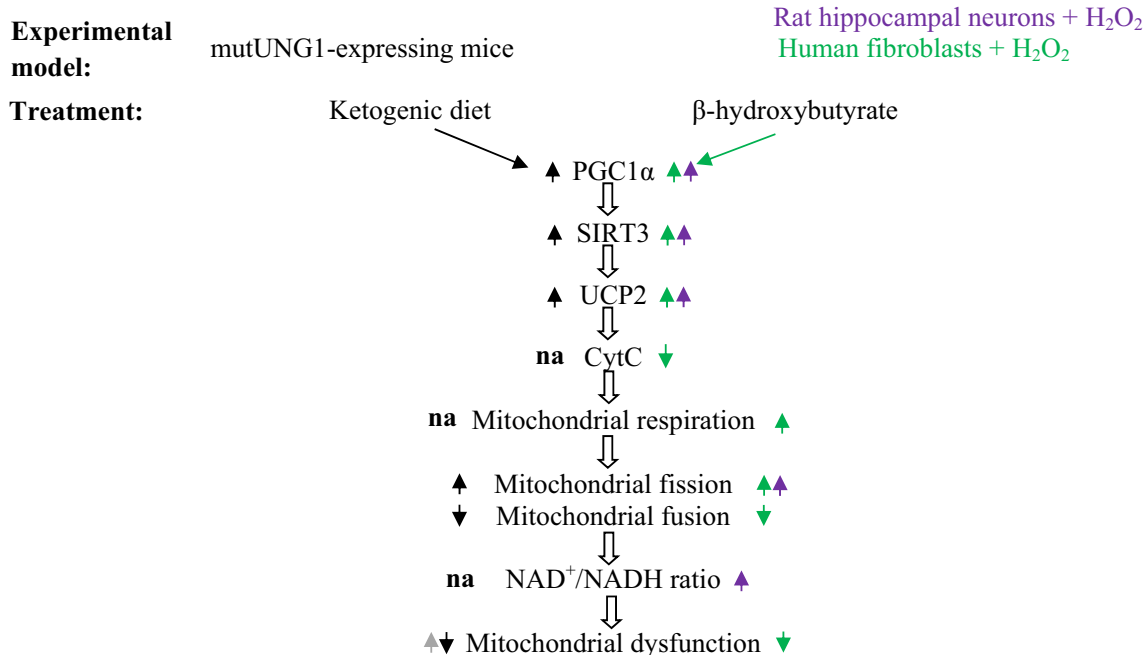


**Fig. 5** Schematic representation of the action of ketones on mitochondria via the “PGC1 $\alpha$ -SIRT3-UCP2 axis”. A KD (left part of figure, black solid arrows) increases the level of the master regulator for mitochondrial biogenesis, PGC1 $\alpha$  (protein Fig. 3a; mRNA Fig. 4a), and ketones upregulate the mitochondrial deacetylase, sirtuin 3 (SIRT3) in mice [41]. The level of UCP2 increases (protein Figs. 1 and 3a; mRNA Fig. 4b), which helps to reduce oxidative stress (OS) [50]. Due to the complex network of interactions, the open arrows do not represent a simple sequence of events. For example, UCP2 may increase SIRT3 to reduce mitochondrial OS and activate PGC1 $\alpha$  [75]. A KD also tends to induce a higher level of mitochondrial fission by increasing the level of Drp1, and to reduce fusion through reducing Mfn1. In cultured human fibroblasts and rat hippocampal neurons (green and purple respectively, right

part of figure),  $\beta$ -hydroxybutyrate ( $\beta$ HB) shows similar molecular effects as a KD, increasing the levels of PGC1 $\alpha$ , SIRT3 and UCP2. The level of NAD<sup>+</sup>/NADH ratio, a measure of mitochondrial activity was significantly elevated by  $\beta$ HB and the opposite effect was exhibited by H<sub>2</sub>O<sub>2</sub>. The mitochondrial respiration was rescued by  $\beta$ HB in H<sub>2</sub>O<sub>2</sub>-exposed fibroblasts. The effects of KD and  $\beta$ HB were beneficial in rescuing mitochondrial damage. (However, KD in sum aggravates mitochondrial dysfunction (grey arrow) in mutUNG1-expressing mice, presumably due to the self-propagating action of mutUNG1 [53], which means that enhanced formation of mitochondria results only in larger masses of malfunctioning mitochondria, which generate increased amounts of ROS when exposed to KD.) Thin solid arrows indicate increase or decrease, *na* not analyzed in the present study

## Compliance with Ethical Standards

**Conflict of interest** The authors have no actual or potential conflicts of interest. All aspects of the research described here were carried out in accordance with the laws of Norway concerning animal research.

## References

- Kann O, Kovacs R (2007) Mitochondria and neuronal activity. *Am J Physiol Cell Physiol* 292:C641–C657
- Yang Y, Ouyang Y, Yang L, Beal MF, McQuibban A, Vogel H, Lu B (2008) Pink1 regulates mitochondrial dynamics through interaction with the fission/fusion machinery. *Proc Natl Acad Sci USA* 105:7070–7075
- Richter C, Park JW, Ames BN (1988) Normal oxidative damage to mitochondrial and nuclear DNA is extensive. *Proc Natl Acad Sci USA* 85:6465–6467
- Larsen NB, Rasmussen M, Rasmussen LJ (2005) Nuclear and mitochondrial DNA repair: similar pathways? *Mitochondrion* 5:89–108
- Wallace DC (1994) Mitochondrial DNA sequence variation in human evolution and disease. *Proc Natl Acad Sci USA* 91:8739–8746
- Anderson CT, Friedberg EC (1980) The presence of nuclear and mitochondrial uracil-DNA glycosylase in extracts of human KB cells. *Nucleic Acids Res* 8:875–888
- Cervenka MC, Henry B, Nathan J, Wood S, Volek JS (2013) Worldwide dietary therapies for adults with epilepsy and other disorders. *J Child Neurol* 28:1034–1040
- Kessler SK, Neal EG, Camfield CS, Kossoff EH (2011) Dietary therapies for epilepsy: future research. *Epilepsy Behav* 22:17–22
- Kossoff EH, Zupec-Kania BA, Rho JM (2009) Ketogenic diets: an update for child neurologists. *J Child Neurol* 24:979–988
- Levy R, Cooper P (2003) Ketogenic diet for epilepsy. *Cochrane Database Syst Rev* 2003:CD001903
- Levy RG, Cooper PN, Giri P (2012) Ketogenic diet and other dietary treatments for epilepsy. *Cochrane Database Syst Rev*. <https://doi.org/10.1002/14651858.CD001903.pub2>
- Villeneuve N, Pinton F, Bahi-Buisson N, Dulac O, Chiron C, Nabbout R (2009) The ketogenic diet improves recently worsened focal epilepsy. *Dev Med Child Neurol* 51:276–281
- Ruskin DN, Svedova J, Cote JL, Sandau U, Rho JM, Kawamura M Jr, Boison D, Masino SA (2013) Ketogenic diet improves core symptoms of autism in BTBR mice. *PLoS ONE* 8:e65021
- Zhao Z, Lange DJ, Voustantiok A, MacGrogan D, Ho L, Suh J, Humala N, Thiyagarajan M, Wang J, Pasinetti GM (2006) A ketogenic diet as a potential novel therapeutic intervention in amyotrophic lateral sclerosis. *BMC Neurosci* 7:29
- Ruskin DN, Ross JL, Kawamura M Jr, Ruiz TL, Geiger JD, Masino SA (2011) A ketogenic diet delays weight loss and does not impair working memory or motor function in the R6/2 1J mouse model of Huntington's disease. *Physiol Behav* 103:501–507
- Van der Auwera I, Wera S, Van Leuven F, Henderson ST (2005) A ketogenic diet reduces amyloid beta 40 and 42 in a mouse model of Alzheimer's disease. *Nutr Metab* 2:28
- Vanitallie TB, Nonas C, Di Rocco A, Boyar K, Hyams K, Heysfield SB (2005) Treatment of Parkinson disease with diet-induced hyperketonemia: a feasibility study. *Neurology* 64:728–730
- Hartman AL, Vining EP (2007) Clinical aspects of the ketogenic diet. *Epilepsia* 48:31–42
- Nordi DR, De Vivo DC (2004) Effects of the ketogenic diet on cerebral energy metabolism. In: Stafstrom CE, Rho JM (eds) *Epilepsy and the ketogenic diet*, 1st edn. Humana Press, Totowa, pp 179–184
- Yudkoff M, Daikhin Y, Nissim I, Nissim I (2004) The ketogenic diet: interactions with brain amino acid handling. In: Stafstrom CE, Rho JM (eds) *Epilepsy and the ketogenic diet*, 1st edn. Humana Press, Totowa, pp 185–200
- Newman JC, Covarrubias AJ, Zhao M, Yu X, Gut P, Ng CP, Huang Y, Haldar S, Verdin E (2017) Ketogenic diet reduces midlife mortality and improves memory in aging mice. *Cell Metab* 26:547–557.e548
- Roberts MN, Wallace MA, Tomilov AA, Zhou Z, Marcotte GR, Tran D, Perez G, Gutierrez-Casado E, Koike S, Knotts TA, Imai DM, Griffey SM, Kim K, Hagopian K, Haj FG, Baar K, Cortopassi GA, Ramsey JJ, Lopez-Dominguez JA (2017) A ketogenic diet extends longevity and healthspan in adult mice. *Cell Metab* 26:539–546.e535
- Halestrap AP, Meredith D (2004) The SLC16 gene family—from monocarboxylate transporters (MCTs) to aromatic amino acid transporters and beyond. *Pflugers Arch* 447:619–628
- Forero-Quintero LS, Deitmer JW, Becker HM (2017) Reduction of epileptiform activity in ketogenic mice: the role of monocarboxylate transporters. *Sci Rep* 7:4900
- Nedergaard J, Cannon B (2003) The 'novel' 'uncoupling' proteins UCP2 and UCP3: what do they really do? Pros and cons for suggested functions. *Exp Physiol* 88:65–84
- Sullivan PG, Rippey NA, Dorenbos K, Concepcion RC, Agarwal AK, Rho JM (2004) The ketogenic diet increases mitochondrial uncoupling protein levels and activity. *Ann Neurol* 55:576–580
- Korshunov SS, Skulachev VP, Starkov AA (1997) High protonic potential actuates a mechanism of production of reactive oxygen species in mitochondria. *FEBS Lett* 416:15–18
- Pecqueur C, Alves-Guerra MC, Gelly C, Levi-Meyrueis C, Couplan E, Collins S, Ricquier D, Bouillaud F, Miroux B (2001) Uncoupling protein 2, in vivo distribution, induction upon oxidative stress, and evidence for translational regulation. *J Biol Chem* 276:8705–8712
- Diano S, Matthews RT, Patrylo P, Yang L, Beal MF, Barnstable CJ, Horvath TL (2003) Uncoupling protein 2 prevents neuronal death including that occurring during seizures: a mechanism for preconditioning. *Endocrinology* 144:5014–5021
- Toda C, Diano S (2014) Mitochondrial UCP2 in the central regulation of metabolism. *Best Pract Res Clin Endocrinol Metab* 28:757–764
- Bechmann I, Diano S, Warden CH, Bartfai T, Nitsch R, Horvath TL (2002) Brain mitochondrial uncoupling protein 2 (UCP2): a protective stress signal in neuronal injury. *Biochem Pharmacol* 64:363–367
- Conti B, Sanchez-Alavez M, Winsky-Sommerer R, Morale MC, Lucero J, Brownell S, Fabre V, Huitron-Resendiz S, Henriksen S, Zorrilla EP, de Lecea L, Bartfai T (2006) Transgenic mice with a reduced core body temperature have an increased life span. *Science* 314:825–828
- Fridell YW, Sanchez-Blanco A, Silvia BA, Helfand SL (2005) Targeted expression of the human uncoupling protein 2 (hUCP2) to adult neurons extends life span in the fly. *Cell Metab* 1:145–152
- Hirose M, Schilf P, Lange F, Mayer J, Reichart G, Maity P, Jöhren O, Schwaninger M, Scharffetter-Kochanek K, Sina C, Sadik CD, Kohling R, Miroux B, Ibrahim SM (2016) Uncoupling protein 2 protects mice from aging. *Mitochondrion* 30:42–50
- Andrews ZB, Horvath B, Barnstable CJ, Elsworth J, Yang L, Beal MF, Roth RH, Matthews RT, Horvath TL (2005) Uncoupling protein-2 is critical for nigral dopamine cell survival in a mouse model of Parkinson's disease. *J Neurosci* 25:184–191

36. Conti B, Sugama S, Lucero J, Winsky-Sommerer R, Wirz SA, Maher P, Andrews Z, Barr AM, Morale MC, Paneda C, Pember-ton J, Gaidarova S, Behrens MM, Beal F, Sanna PP, Horvath T, Bartfai T (2005) Uncoupling protein 2 protects dopaminergic neu-rons from acute 1,2,3,6-methyl-phenyl-tetrahydropyridine toxicity. *J Neurochem* 93:493–501
37. Mattiasson G, Shamloo M, Gido G, Mathi K, Tomasevic G, Yi S, Warden CH, Castilho RF, Melcher T, Gonzalez-Zulueta M, Nikolich K, Wieloch T (2003) Uncoupling protein-2 prevents neuronal death and diminishes brain dysfunction after stroke and brain trauma. *Nat Med* 9:1062–1068
38. Bough K (2008) Energy metabolism as part of the anticonvulsant mechanism of the ketogenic diet. *Epilepsia* 49(Suppl 8):91–93
39. Srivastava S, Baxa U, Niu G, Chen X, Veech RL (2013) A ketogenic diet increases brown adipose tissue mitochondrial pro-teins and UCP1 levels in mice. *IUBMB Life* 65:58–66
40. Hutfles LJ, Wilkins HM, Koppel SJ, Weidling IW, Selfridge JE, Tan E, Thyfault JP, Slawson C, Fenton AW, Zhu H, Swerdlow RH (2017) A bioenergetics systems evaluation of ketogenic diet liver effects. *Appl Physiol Nutr Metab* 42:955–962
41. Yin J, Han P, Tang Z, Liu Q, Shi J (2015) Sirtuin 3 mediates neuroprotection of ketones against ischemic stroke. *J Cereb Blood Flow Metab* 35:1783–1789
42. Rardin MJ, Newman JC, Held JM, Cusack MP, Sorensen DJ, Li B, Schilling B, Mooney SD, Kahn CR, Verdin E, Gibson BW (2013) Label-free quantitative proteomics of the lysine acetylo-me in mitochondria identifies substrates of SIRT3 in metabolic path-ways. *Proc Natl Acad Sci USA* 110:6601–6606
43. Pagel-Langenickel I, Bao J, Joseph JJ, Schwartz DR, Mantell BS, Xu X, Raghavachari N, Sack MN (2008) PGC-1alpha integrates insulin signaling, mitochondrial regulation, and bioenergetic func-tion in skeletal muscle. *J Biol Chem* 283:22464–22472
44. Lomb DJ, Laurent G, Haigis MC (2010) Sirtuins regu-late key aspects of lipid metabolism. *Biochim Biophys Acta* 1804:1652–1657
45. Ansari A, Rahman MS, Saha SK, Saikot FK, Deep A, Kim KH (2017) Function of the SIRT3 mitochondrial deacetylase in cel-lular physiology, cancer, and neurodegenerative disease. *Aging Cell* 16:4–16
46. Su J, Liu J, Yan XY, Zhang Y, Zhang JJ, Zhang LC, Sun LK (2017) Cytoprotective effect of the UCP2-SIRT3 signaling path-way by decreasing mitochondrial oxidative stress on cerebral ischemia-reperfusion injury. *Int J Mol Sci* 18
47. Lauritzen KH, Moldestad O, Eide L, Carlsen H, Nesse G, Storm JF, Mansuy IM, Bergersen LH, Klungland A (2010) Mitochon-drial DNA toxicity in forebrain neurons causes apoptosis, neuro-degeneration, and impaired behavior. *Mol Cell Biol* 30:1357–1367
48. Dianov GL, Sleeth KM, Dianova II, Allinson SL (2003) Repair of abasic sites in DNA. *Mutat Res* 531:157–163
49. Pinz KG, Shibusaki S, Bogenhagen DF (1995) Action of mito-chondrial DNA polymerase gamma at sites of base loss or oxida-tive damage. *J Biol Chem* 270:9202–9206
50. Lauritzen KH, Dalhus B, Storm JF, Bjoras M, Klungland A (2011) Modeling the impact of mitochondrial DNA damage in forebrain neurons and beyond. *Mech Ageing Dev* 132:424–428
51. Loeb LA, Wallace DC, Martin GM (2005) The mitochondrial theory of aging and its relationship to reactive oxygen species damage and somatic mtDNA mutations. *Proc Natl Acad Sci USA* 102:18769–18770
52. Nicholls DG (2008) Oxidative stress and energy crises in neuronal dysfunction. *Ann NY Acad Sci* 1147:53–60
53. Lauritzen KH, Hasan-Olive MM, Regnell CE, Kleppa L, Scheibye-Knudsen M, Gjedde A, Klungland A, Bohr VA, Storm-Mathisen J, Bergersen LH (2016) A ketogenic diet accelerates neurodegeneration in mice with induced mitochondrial DNA tox-icity in the forebrain. *Neurobiol Aging* 48:34–47
54. Bergersen LH, Storm-Mathisen J, Gundersen V (2008) Immuno-gold quantification of amino acids and proteins in complex subcel-lular compartments. *Nat Protoc* 3:144–152
55. Marosi K, Kim SW, Moehl K, Scheibye-Knudsen M, Cheng A, Cutler R, Camandola S, Mattson MP (2016) 3-Hydroxybutyrate regulates energy metabolism and induces BDNF expression in cerebral cortical neurons. *J Neurochem* 139:769–781
56. Reddy PH, Shirendeb UP (2012) Mutant huntingtin, abnormal mitochondrial dynamics, defective axonal transport of mitochon-dria, and selective synaptic degeneration in Huntington's disease. *Biochim Biophys Acta* 1822:101–110
57. Wang Q, Zhang M, Liang B, Shirwany N, Zhu Y, Zou MH (2011) Activation of AMP-activated protein kinase is required for ber-berine-induced reduction of atherosclerosis in mice: the role of uncoupling protein 2. *PLoS ONE* 6:e25436
58. Coyle CH, Kader KN (2007) Mechanisms of H<sub>2</sub>O<sub>2</sub>-induced oxida-tive stress in endothelial cells exposed to physiologic shear stress. *ASAJO J* 53:17–22
59. Olichon A, Guillou E, Delettre C, Landes T, Arnaune-Pelloquin L, Emorine LJ, Mils V, Daloyau M, Hamel C, Amati-Bonneau P, Bonneau D, Reynier P, Lenaers G, Belenguer P (2006) Mito-chondrial dynamics and disease, OPA1. *Biochim Biophys Acta* 1763:500–509
60. Lu B (2009) Mitochondrial dynamics and neurodegeneration. *Curr Neurol Neurosci Rep* 9:212–219
61. Kuei C, Yu J, Zhu J, Wu J, Zhang L, Shih A, Mirzadegan T, Lovenberg T, Liu C (2011) Study of GPR81, the lactate recep-tor, from distant species identifies residues and motifs critical for GPR81 functions. *Mol Pharmacol* 80:848–858
62. Richard D, Clavel S, Huang Q, Sanchis D, Ricquier D (2001) Uncoupling protein 2 in the brain: distribution and function. *Bio-chem Soc Trans* 29:812–817
63. Simuni T, Sethi K (2008) Nonmotor manifestations of Parkinson's disease. *Ann Neurol* 64(Suppl 2):S65–S80
64. Ahola-Erkkila S, Carroll CJ, Peltola-Mjosund K, Tulkki V, Mattila I, Seppanen-Laakso T, Oresic M, Tynyismaa H, Suomalainen A (2010) Ketogenic diet slows down mitochondrial myopathy pro-gression in mice. *Hum Mol Genet* 19:1974–1984
65. Al-Zaid NS, Dashti HM, Mathew TC, Juggi JS (2007) Low car-bohydrate ketogenic diet enhances cardiac tolerance to global ischaemia. *Acta Cardiol* 62:381–389
66. Bough KJ, Wetherington J, Hassel B, Pare JF, Gawryluk JW, Greene JG, Shaw R, Smith Y, Geiger JD, Dingleline RJ (2006) Mitochondrial biogenesis in the anticonvulsant mechanism of the ketogenic diet. *Ann Neurol* 60:223–235
67. Kim DK, Heineman FW, Balaban RS (1991) Effects of beta-hydroxybutyrate on oxidative metabolism and phosphorylation potential in canine heart in vivo. *Am J Physiol* 260:H1767–H1773
68. Tieu K, Perier C, Caspersen C, Teismann P, Wu DC, Yan SD, Naini A, Vila M, Jackson-Lewis V, Ramasamy R, Przedborski S (2003) D-beta-hydroxybutyrate rescues mitochondrial respira-tion and mitigates features of Parkinson disease. *J Clin Invest* 112:892–901
69. Sampson M, Lathen D, Dallon B, Draney C, Ray J, Kener K, Parker B, Witt J, Gibbs J, Tessem JS, Bikman BT (2017) Beta-hydroxybutyrate favorably alters b-cell survival and mitochondrial bioenergetics. *FASEB J* 31:883.888
70. Masuda R, Monahan JW, Kashiwaya Y (2005) D-beta-hydroxybu-tyrate is neuroprotective against hypoxia in serum-free hippocam-pal primary cultures. *J Neurosci Res* 80:501–509
71. Jornayvaz FR, Jurczak MJ, Lee HY, Birkenfeld AL, Frederick DW, Zhang D, Zhang XM, Samuel VT, Shulman GI (2010) A high-fat, ketogenic diet causes hepatic insulin resistance in mice, despite increasing energy expenditure and preventing weight gain. *Am J Physiol Endocrinol Metab* 299:E808–E815

72. Chan DC (2006) Mitochondrial fusion and fission in mammals. *Annu Rev Cell Dev Biol* 22:79–99
73. Chen H, Chan DC (2006) Critical dependence of neurons on mitochondrial dynamics. *Curr Opin Cell Biol* 18:453–459
74. Brenmoehl J, Hoefflich A (2013) Dual control of mitochondrial biogenesis by sirtuin 1 and sirtuin 3. *Mitochondrion* 13:755–761
75. Shimazu T, Hirschey MD, Hua L, Dittenhafer-Reed KE, Schwer B, Lombard DB, Li Y, Bunkenborg J, Alt FW, Denu JM, Jacobson MP, Verdin E (2010) SIRT3 deacetylates mitochondrial 3-hydroxy-3-methylglutaryl CoA synthase 2 and regulates ketone body production. *Cell Metab* 12:654–661
76. Liu J, Li D, Zhang T, Tong Q, Ye RD, Lin L (2017) SIRT3 protects hepatocytes from oxidative injury by enhancing ROS scavenging and mitochondrial integrity. *Cell Death Dis* 8:e3158
77. Ding Y, Yang H, Wang Y, Chen J, Ji Z, Sun H (2017) Sirtuin 3 is required for osteogenic differentiation through maintenance of PGC-1 $\alpha$ -SOD2-mediated regulation of mitochondrial function. *Int J Biol Sci* 13:254–264
78. Elamin M, Ruskin DN, Masino SA, Sacchetti P (2017) Ketone-based metabolic therapy: is increased NAD(+) a primary mechanism? *Front Mol Neurosci* 10:377

## Affiliations

Md Mahdi Hasan-Olive<sup>1,2,3</sup> · Knut H. Lauritzen<sup>1,4</sup> · Mohammad Ali<sup>5</sup> · Lene Juel Rasmussen<sup>3</sup> · Jon Storm-Mathisen<sup>1</sup> · Linda H. Bergersen<sup>1,2,3</sup> 

<sup>1</sup> Synaptic Neurochemistry and Amino Acid Transporter Laboratory, Division of Anatomy and CMBN/SERTA Healthy Brain Ageing Center, Institute of Basic Medical Sciences, University of Oslo, Oslo, Norway

<sup>2</sup> Brain and Muscle Energy Group, Electron Microscopy Laboratory, Institute of Oral Biology, University of Oslo, Oslo, Norway

<sup>3</sup> Center for Healthy Aging, Department of Neurosciences and Pharmacology, Faculty of Health Sciences, University of Copenhagen, Copenhagen, Denmark

<sup>4</sup> Research Institute of Internal Medicine, Oslo University Hospital Rikshospitalet, Oslo, Norway

<sup>5</sup> Department of Biochemistry, Sir Salimullah Medical College & Mitford Hospital, Dhaka, Bangladesh